

**STUDY ON CRYSTALLIZATION KINETICS AND SUBSEQUENT
MELTING BEHAVIOR OF POLYMERS WITH DIFFERENT MOLECULAR
CHARACTERISTICS AND POLYMERS FILLED WITH VARIOUS TYPES
OF ADDITIVES**



Pakin Thanomkiat

A Dissertation Submitted in Partial Fulfilment of the Requirements
for the Degree of Doctor of Philosophy
The Petroleum and Petrochemical College, Chulalongkorn University
in Academic Partnership with
The University of Michigan, The University of Oklahoma,
and Case Western Reserve University

2007

502077

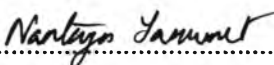
Thesis Title: Study on Crystallization Kinetics and Subsequent Melting Behavior of Polymer with Different Molecular Characteristics and Polymer Filled with Various Types of Additives

By: Pakin Thanomkiat

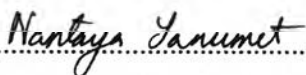
Program: Polymer Science

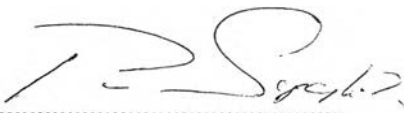
Thesis Advisors: Assoc.Prof. Pitt Supaphol
Prof. Stephen Z.D. Cheng

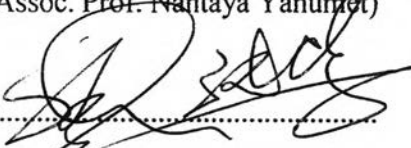
Accepted by the Petroleum and Petrochemical College, Chulalongkorn University, in partial fulfilment of the requirements for the Degree of Doctor of Philosophy.

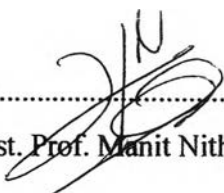

..... College Director
(Assoc. Prof. Nantaya Yanumet)

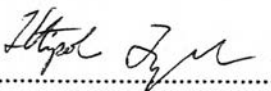
Thesis Committee:



.....
(Assoc. Prof. Nantaya Yanumet)


.....
(Assoc. Prof. Pitt Supaphol)


.....
(Prof. Stephen Z.D.Cheng)


.....
(Assist. Prof. Manit Nithithanakul)


.....
(Assoc. Prof. Ittipol Jangchud)


.....
(Assoc. Prof. Taweechai Amornsakchai)

ABSTRACT

4482001063: Polymer Science Program

Pakin Thanomkiat: Study on Crystallization Kinetics and Subsequent Melting Behavior of Polymers with Different Molecular Characteristics and Polymers Filled with Various Types of Additives.

Thesis Advisors: Assoc. Prof. Pitt Supaphol, and Prof. Stephen Z.D. Cheng 159 pp.

Keywords: Equilibrium melting temperature/ Crystallization kinetics/ Macrokinetic model/ Syndiotactic polypropylene/ Pigment/ TiO₂ nanoparticles

Crystallization and subsequent melting behavior for six syndiotactic polypropylene (sPP) resins having different molecular characteristics, medium-density polyethylene (MDPE) filled with 3 types of pigments (i.e. diarylide, phthalocyanine, and quinacridone), and isotactic polypropylene (iPP) filled with titanium(IV)oxide (TiO₂) with 3 different surface modifications were investigated by differential scanning calorimetry (DSC). The crystallization kinetics were analyzed based on various macrokinetic models, i.e. Avrami, Malkin, Urbanovici-Segal, Ozawa, and Ziabicki. The equilibrium melting temperature (T_m^0) was also estimated based on the linear and non-linear Hoffman-Weeks extrapolative methods. In general, the estimated T_m^0 values were found to increase with increasing syndiotacticity level. By comparing these values along with the values obtained from literature, the T_m^0 value for a perfect sPP can be estimated. The subsequent melting behavior of sPP after crystallization process exhibited either a single melting endotherm or double melting endotherms. For the crystallization behavior of pigmented MDPE resins, it was found that diarylide could be the only pigment that was effective in accelerating the crystallization processes compared to other two pigments.

บทคัดย่อ

ภคิน ถนอมเกียรติ : การศึกษาพฤติกรรมการตกผลึกและการหลอมเหลวของผลึกที่เกิดขึ้นของพอลิเมอร์ที่มีคุณลักษณะของโมเลกุลต่างกัน และพอลิเมอร์ที่มีการใส่สารเติมชนิดต่างๆ (Study on Crystallization Kinetics and Subsequent Melting Behavior of Polymers with Different Molecular Characteristics and Polymer Filled with Various Types of Additives) อ. ที่ปรึกษา : รศ. ดร. พิชญ์ สุภผล และ ศ.สตีเฟน เสง 159 หน้า

พฤติกรรมการตกผลึกและการหลอมเหลว ของซินติโอแทคติกพอลิโพรพิลีน ที่มีคุณลักษณะของโมเลกุลต่าง ๆ กัน พอลิเอทิลีนความหนาแน่นปานกลางที่เติมด้วยรงควัตถุต่างชนิดสามชนิด (ได้แก่ ไคอะริลไลด์ ฟะทาโลไซยานิน และควินอะคริโตน) และไอโซแทคติกพอลิโพรพิลีน ที่เติมด้วยไทเทเนียมไดออกไซด์ที่มีอนุภาคขนาดนาโนเมตร และมีคุณสมบัติของพื้นผิวต่างกันสามชนิด ได้รับการศึกษาโดยอาศัยเทคนิคดิฟเฟอเรนเชียล สแกนนิ่ง แคลอริเมทรี ซึ่งสามารถนำผลการทดลองจากเทคนิคดังกล่าวมาวิเคราะห์ โดยอาศัยโมเดลต่าง ๆ ได้แก่ อาฟรามิ มาลคิน เออร์บานอวิช-เซกาล โอซาวา และ ไซอะบิกกิ ซึ่งสามารถทำให้สามารถเปรียบเทียบอัตราการตกผลึก รวมทั้งกลไกการตกผลึกของพอลิเมอร์ต่าง ๆ ดังกล่าวได้ จุดหลอมเหลวสมดุลของพอลิเมอร์สามารถหาได้จากวิธีการของฮอฟแมน-วีก ซึ่งพบว่า เมื่อปริมาณซินติโอแทคติกมากขึ้น ค่าจุดหลอมเหลวสมดุลจะมีค่าเพิ่มขึ้น นอกจากนี้ ยังทำให้ประมาณค่าของจุดหลอมเหลวสมดุลสำหรับซินติโอแทคติกพอลิโพรพิลีนที่มีปริมาณซินติโอแทคติกร้อยละหนึ่งได้ สำหรับรงควัตถุที่มีผลต่อการตกผลึกของพอลิเอทิลีนนั้น พบว่า สารไคอะริลไลด์ เป็นสารที่สามารถเร่งการตกผลึกของพอลิเอทิลีนได้ดีที่สุด ในส่วนของการตกผลึกของไอโซแทคติกพอลิโพรพิลีน ที่เติมด้วย ไทเทเนียมไดออกไซด์ที่มีอนุภาคขนาดนาโนเมตร พบว่า ไททาเนียมไดออกไซด์ ที่ฉาบพื้นผิวด้วยซิลิกอนไดออกไซด์ จะสามารถช่วยให้เกิดการตกผลึกของพอลิโพรพิลีนได้ดีกว่า ไททาเนียมไดออกไซด์ที่ไม่ได้ผ่านการฉาบเคลือบผิว แต่ไททาเนียมไดออกไซด์ที่ฉาบด้วยกรดไขมัน มีแนวโน้มในการทำให้กระบวนการตกผลึกของพอลิโพรพิลีนช้าลง

ACKNOWLEDGEMENTS

The author is grateful for the partial scholarship and partial funding of the thesis work provided by the Petroleum and Petrochemical College; and the National Excellence Center for Petroleum, Petrochemicals, and Advanced Materials, Thailand.

This work was also supported in parts by the Thailand Research Fund (TRF) through the Royal Golden Jubilee PhD Program (2.L.CU/45/H.1).

Ratchanu Buhngachat was acknowledged for her contribution in preparing the pigmented MDPE samples investigated in this work.

Finally, Assoc. Prof. Pitt Supaphol was also acknowledged for his advices throughout all the works presented in this dissertation.

TABLE OF CONTENTS

	PAGE
Title Page	i
Abstract (in English)	iii
Abstract (in Thai)	iv
Acknowledgements	v
Table of Contents	vi
List of Tables	ix
List of Figures	xiii
Abbreviations	xix
List of Symbols	xx
 CHAPTER	
I INTRODUCTION	1
 II LITERATURE REVIEW	 4
 III EXPERIMENTAL	 16
 IV INFLUENCE OF MOLECULAR CHARACTERISTICS ON OVERALL ISOTHERMAL MELT- CRYSTALLIZATION BEHAVIOR AND EQUILIBRIUM MELTING TEMPERATURE OF SYNDIOTACTIC POLYPROPYLENE	 24
4.1 Abstract	24
4.2 Introduction	24
4.3 Theoretical Background	25
4.4 Experimental	28
4.5 Results and Discussion	31
4.6 Conclusions	53

CHAPTER	PAGE
4.7 Acknowledgements	54
4.8 References	54
V INFLUENCE OF MOLECULAR CHARACTERISTICS ON NON-ISOTHERMAL MELT-CRYSTALLIZATION KINETICS OF SYNDIOTACTIC POLYPROPYLENE	56
5.1 Abstract	56
5.2 Introduction	56
5.3 Theoretical Background	57
5.4 Experimental	62
5.5 Results and Discussion	64
5.6 Conclusions	84
5.7 Acknowledgements	85
5.8 References	85
VI NON-ISOTHERMAL MELT-CRYSTALLIZATION AND SUBSEQUENT MELTING BEHAVIOR OF PIGMENTED MEDIUM-DENSITY POLYETHYLENE	87
6.1 Abstract	87
6.2 Introduction	87
6.3 Theoretical Background	88
6.4 Experimental	89
6.5 Results and Discussion	92
6.6 Conclusions	116
6.7 Acknowledgements	116
6.8 References	116

CHAPTER	PAGE
VII NON-ISOTHERMAL MELT-CRYSTALLIZATION AND MECHANICAL PROPERTIES OF TITANIUM(IV)OXIDE NANOPARTICLE-FILLED ISOTACTIC POLYPROPYLENE	118
7.1 Abstract	118
7.2 Introduction	119
7.3 Theoretical Background	120
7.4 Experimental	121
7.5 Results and Discussion	124
7.6 Conclusions	153
7.7 Acknowledgements	153
7.8 References	154
VIII CONCLUSIONS AND RECOMMENDATIONS	155
CURRICULUM VITAE	158

LIST OF TABLES

TABLE		PAGE
CHAPTER III		
3.1	Molecular characteristics of sPP#9 to sPP#14	17
3.2	Specific properties of the TiO ₂ nanoparticles	18
CHAPTER IV		
4.1	Molecular characteristics of sPP# 9-14 and the equilibrium melting temperature (T_m^0) based on linear and nonlinear Hoffman-Weeks extrapolation	29
4.2	Characteristic data of the melting endotherm after isothermal crystallization of sPP# 9-14	34
4.3	Isothermal crystallization kinetic parameters of sPP# 9-14 based on Avrami analysis	42
4.4	Isothermal crystallization kinetic parameters of sPP# 9-14 based on Malkin analysis	46
4.5	Isothermal crystallization kinetic parameters of sPP# 9-14 based on Urbanovici-Segal analysis	48
CHAPTER V		
5.1	Molecular characteristics of sPP# 9 to sPP#14 and the estimated equilibrium melting temperature (T_m^0) based on linear Hoffman-Weeks extrapolative method	63
5.2	Characteristic data from non-isothermal melt-crystallization exotherms for sPP# 9 to sPP#14	67
5.3	Quantitative analysis of the relative crystallinity functions of time which were converted from non-isothermal melt-crystallization of sPP#9 to sPP#14	71

TABLE	PAGE
5.4 y -intercept, slope, and the r^2 values of regression lines drawn through plots of $\ln(t_0)$ against $\ln(\phi)$ for various relative crystallinity values	73
5.5 Characteristic data of subsequent melting endotherms after non-isothermal melt-crystallization for sPP#9 to sPP#14	75
5.6 Non-isothermal melt-crystallization kinetic parameters for sPP# 9 to sPP#14 based on Avrami analysis	77
5.7 Non-isothermal melt-crystallization kinetic parameters for sPP# 9 to sPP#14 based on Urbanovici-Segal analysis	78
5.8 Non-isothermal melt-crystallization kinetic parameters for sPP# 9 to sPP#14 based on Ozawa analysis	81
5.9 Non-isothermal melt-crystallization kinetic parameters for sPP# 9 to sPP#14 based on Ziabicki's kinetic crystallizability analysis	82
5.10 Effective energy barrier for overall non-isothermal melt-crystallization of sPP#9 to sPP#14 based on the differential iso-conversional method of Friedman	83
 CHAPTER VI 	
6.1 Characteristic data of non-isothermal melt-crystallization exotherms for neat MDPE and pigmented MDPE	97
6.2 Quantitative analysis of the relative crystallinity as a functions of time for neat MDPE	100
6.3 Quantitative analysis of the relative crystallinity as a functions of time for MDPE filled with various amount of diarylide	102
6.4 Quantitative analysis of the relative crystallinity as a functions of time for MDPE filled with various amount of phthalocyanine	103

TABLE	PAGE
6.5 Quantitative analysis of the relative crystallinity as a functions of time for MDPE filled with various amount of quinacridone	104
6.6 y -intercept, slope, and the r^2 values of regression lines drawn through plots of $\ln(t_\theta)$ against $\ln(\phi)$ for various θ values	105
6.7 Characteristic data of subsequent melting endotherms after non-isothermal melt-crystallization for neat and pigmented MDPE	109
6.8 Non-isothermal melt-crystallization kinetics for pure MDPE and pigment-added MDPE based on Avrami analysis for primary crystallization process (covering the θ range of 0.1-0.4)	112
6.9 Non-isothermal melt-crystallization kinetics for pure MDPE and pigment-added MDPE based on Avrami analysis for secondary crystallization process (covering the θ range of 0.6-0.9)	114
 CHAPTER VII 	
7.1 Specific properties of the TiO ₂ nanoparticles	122
7.2 Characteristic data of non-isothermal melt-crystallization exotherms for neat and TiO ₂ -filled iPP	126
7.3 Quantitative analysis of the relative crystallinity as a functions of time for neat iPP	132
7.4 Quantitative analysis of the relative crystallinity as a functions of time for iPP filled with CYU201	133
7.5 Quantitative analysis of the relative crystallinity as a functions of time for iPP filled with CYU202	134

TABLE	PAGE
7.6 Quantitative analysis of the relative crystallinity as a functions of time for iPP filled with CYU203	135
7.7 y -intercept, slope, and the r^2 values of regression lines drawn through plots of $\ln(t_\theta)$ versus $\ln(\phi)$ for various θ values	136
7.8 Characteristic data of subsequent melting endotherms after non-isothermal melt-crystallization for neat and TiO ₂ -filled iPP	143
7.9 Non-isothermal melt-crystallization kinetics for neat and TiO ₂ -filled based on Avrami analysis over the crystallinity range of 10 to 80%	146

LIST OF FIGURES

FIGURE		PAGE
CHAPTER II		
2.1	The proposed polymer crystal morphologies (a) “fringed-micelle model” (b) “folded-chain lamellar model” and (c) “spherulitic morphology”	5
CHAPTER III		
3.1	Chemical structure of the three pigments investigated: (a) quinacridone or ‘Pigment Red 122’, (b) phthalocyanine or ‘Pigment Blue 25’, and (c) diarylide or ‘Pigment Yellow 83’	18
CHAPTER IV		
4.1	(a) Isothermal melt-crystallization exotherms for sPP#10 observed at different crystallization temperatures, ranging from 88 to 108°C.	32
	(b) Subsequent melting thermograms for sPP#10 observed during subsequent heating at a heating rate of 20°C min ⁻¹ after isothermal melt-crystallization at different crystallization temperatures, ranging from 88 to 108°C.	33
4.2	Observed melting temperature as a function of crystallization temperature for sPP#9. The raw data are shown as geometrical points. The dotted line represents the linear Hoffman-Weeks extrapolation and the solid line represents the non-linear Hoffman-Weeks extrapolation.	36
4.3	Determination of the equilibrium melting temperature for a perfect sPP (i.e. sPP of 100% syndiotacticity level) by extrapolation of the observed equilibrium melting	

FIGURE

PAGE

- temperatures (i.e. T_m^{LHW}) of the sPP resins shown in Table 4.1 as a function of the racemic pentad content. Keys: data obtained from this work (●) and from the literature (○). 38
- 4.4 Determination of the equilibrium melting temperature for a perfect sPP by means of a modified Flory's theory for the depression of the equilibrium melting temperature in copolymers through the plot of $1/T_m^{LHW}$ versus $-\ln p_r$, where p_r is the racemic dyad content. Keys: data obtained from this work (●) and from the literature (○). 39
- 4.5 (a) Relative crystallinity as a function of crystallization time for sPP#11 observed at different crystallization temperatures, ranging from 92 to 110°C. The experimental data, shown as various geometrical points, were fitted to the Avrami macrokinetic models, in which the best fits are shown as solid lines. 41
- (b) Relative crystallinity as a function of crystallization time for sPP#11 observed at different crystallization temperatures, ranging from 92 to 110°C. The experimental data, shown as various geometrical points, were fitted to the Malkin macrokinetic models, in which the best fits are shown as solid lines. 45
- (c) Relative crystallinity as a function of crystallization time for sPP#11 observed at different crystallization temperatures, ranging from 92 to 110°C. The experimental data, shown as various geometrical points, were fitted to the Urbanovici-Segal macrokinetic models, in which the best fits are shown as solid lines. 50

FIGURE	PAGE	
4.6	Reciprocal half-times of crystallization as a function of crystallization temperature for (●) sPP#9, (○) sPP#10, (▼) sPP#11, (▽) sPP#12, (■) sPP#13, and (□) sPP#14.	51
4.7	Various crystallization rate parameters shown as various geometrical points as a function of crystallization temperature for sPP#12 observed at different crystallization temperatures, ranging from 74 to 96°C.	52
CHAPTER V		
5.1	(a) Non-isothermal melt-crystallization exotherm of sPP#10 observed for seven different cooling rates, ranging from 5 to 40°C min ⁻¹ .	65
	(b) Subsequent melting endotherm of sPP#10 after non-isothermal melt-crystallization at corresponding cooling rates. The subsequent melting endotherm was recorded at a heating rate of 20°C min ⁻¹	66
5.2	(a) Relative crystallinity as a function of time of sPP#11 observed for seven different cooling rates, ranging from 5 to 40°C min ⁻¹ . The raw experimental data are shown as various geometrical points; whereas the model predictions based on Avrami model are shown as solid lines.	68
	(b) Relative crystallinity as a function of time of sPP#11 observed for seven different cooling rates, ranging from 5 to 40°C min ⁻¹ . The raw experimental data are shown as various geometrical points; whereas the model predictions based on Urbanovici-Segal model are shown as solid lines.	69

FIGURE	PAGE
5.3 Crystallization time at various relative crystallinity values as a function of cooling rate for sPP#10. The inset figure shows a relationship between apparent total crystallization period and cooling rate in a log-log plot.	70
5.4 Relationship between crystallization time at various relative crystallinity values and cooling rate in a log-log plot for sPP#10.	74
5.5 Typical Ozawa analysis based on non-isothermal melt-crystallization data of sPP#13.	80
 CHAPTER VI 	
6.1 Chemical structure of the three pigments investigated: (a) quinacridone or 'Pigment Red 122', (b) phthalocyanine or 'Pigment Blue 25', and (c) diarylide or 'Pigment Yellow 83'.	90
6.2 (a) Non-isothermal melt-crystallization exotherm of MDPE filled with 0.1 phr of phthalocyanine (PB01) at six different cooling rates ranging from 5 to 30°C min ⁻¹	93
(b) Corresponding subsequent melting endotherm recorded at a heating rate of 20°C min ⁻¹	94
6.3 (a) Non-isothermal melt-crystallization exotherm of neat and pigmented MDPE recorded at a cooling rate of 10°C min ⁻¹	95
(b) Corresponding subsequent melting endotherm recorded at a heating rate of 20°C min ⁻¹ .	96
6.4 Relative crystallinity as a function of time of MDPE filled with 0.1 phr of diarylide (PY01) at six different cooling rates ranging from 5 to 30°C min ⁻¹ .	99

FIGURE	PAGE
6.5 Crystallization time at various relative crystallinity values as a function of cooling rate for MDPE filled with 0.1 phr of quinacridone (PR01). The inset figure shows a relationship between apparent total crystallization period and cooling rate in a log-log plot.	101
6.6 Crystallization time at various relative crystallinity values as a function of cooling rate in a log-log plot for MDPE filled with 0.1 phr of quinacridone (PR01).	108
6.7 Typical Avrami analysis for MDPE filled with 0.1 phr of diarylide (PY01).	111

CHAPTER VII

7.1 Non-isothermal melt-crystallization exotherm of neat iPP at six different cooling rates.	125
7.2 Non-isothermal melt-crystallization exotherm of neat and TiO ₂ -filled iPP recorded at a cooling rate of 10 ⁰ C min ⁻¹ .	128
7.3 Non-isothermal melt-crystallization exotherms of iPP filled with 30wt% CYU202 at six different cooling rates.	130
7.4 Relative crystallinity as a function of time for iPP filled with 5wt% CYU202 at six different cooling rates after excluding an induction period.	131
7.5 Crystallization time at various relative crystallinity values as a function of cooling rate for neat iPP. The inset figure shows a relationship between apparent total crystallization period and cooling rate in a log-log plot.	136
7.6 Crystallization time at various relative crystallinity values as a function of cooling rate in a log-log plot for neat iPP.	137

FIGURE		PAGE
7.7	Subsequent melting endotherm (recorded at $10^{\circ}\text{C min}^{-1}$) of neat iPP after non-isothermal melt-crystallization at six different cooling rates.	141
7.8	Subsequent melting endotherm (recorded at $10^{\circ}\text{C min}^{-1}$) of iPP filled with 20wt% CYU203 after non-isothermal melt-crystallization at six different cooling rates.	142
7.9	Typical Avrami analysis according to the relative crystallinity as a function of time for neat iPP after non-isothermal melt-crystallization at six different cooling rates.	148
7.10	Tensile strength at yield for neat and TiO_2 -filled iPP	150
7.11	Young's modulus for neat and TiO_2 -filled iPP.	150
7.12	Elongation at yield for neat and TiO_2 -filled iPP.	151
7.13	Impact resistance for neat and TiO_2 -filled iPP.	151
7.14	Flexural strength for neat and TiO_2 -filled iPP.	152
7.15	Flexural modulus for neat and TiO_2 -filled iPP.	152

ABBREVIATIONS

sPP	syndiotactic polypropylene
iPP	isotactic polypropylene
MDPE	medium-density polyethylene
DSC	different scanning calorimetry
NMR	nuclear magnetic resonance
LHW	linear Hoffman-Weeks extrapolation method
NLHW	non-linear Hoffman-Weeks extrapolation method
PY	pigment yellow (diarylide C.I.21108)
PB	pigment blue (phthalocyanine C.I.74160)
PR	pigment red (quinacridone C.I.73915)

LIST OF SYMBOLS

t	time
T	temperature
T_c	crystallization temperature
T_m	melting temperature
T_m^0	equilibrium melting temperature
ΔT_c	degree of undercooling defined as $T_m^0 - T_c$
$\theta(t)$	relative crystallinity function of time
$\theta(T)$	relative crystallinity function of temperature
dH_c	instantaneous enthalpy of crystallization released at an arbitrary crystallization time
ΔH_c	enthalpy of crystallization released over the course of crystallization period
G	linear growth rate of crystal
I	primary nucleation rate
K_A	Avrami rate constant
n_A	Avrami exponent
C_0	Malkin exponent
C_1	Malkin rate constant
K_{US}	Urbanovici-Segal rate constant
n_{US}	Urbanovici-Segal exponent
r	parameter in Urbanovici-Segal macrokinetics model which satisfies the condition $r > 0$
K_O	Ozawa rate constant
n_O	Ozawa exponent
ϕ	cooling rate
$K(T)$	temperature dependent crystallization rate function
K_{max}	maximum crystallization rate

T_{\max}	the temperature which exhibit the maximum crystallization rate
D	the width at the half-height of the crystallization rate function of temperature
G_z	Ziabicki's crystallizability
G_ϕ	crystallizability at an arbitrary cooling rate
$\dot{\theta}_\phi(T)$	derivation function of the relative crystallinity as a function of temperature
$\dot{\theta}_{\max, \phi}$	the maximum crystallization rate of the derivation function of the relative crystallinity
D_ϕ	the width at half-height of the derivation function of the relative crystallinity
σ	lateral surface free energy of crystal lamellae
σ_e	fold surface free energy of crystal lamellae
l	crystal lamellar thickness
l_{\min}	the minimum lamellar thickness needed to form a thermodynamically stable nucleus
l_g^*	critical lamellar thickness to form a thermodynamically stable nucleus at the fastest rate
δl	the increment above l_{\min} to give l_g^*
k	Boltzman constant
β^m	thickening coefficient
σ_e^{GT}	the basal interfacial free energy associated with nuclei of critical size including the extra lateral surface energy due to fold protrusion and the mixing entropy associated with stems of different lengths
σ_e^1	the interfacial energy associated with the formation of the basal plane of the initial crystals
ΔH_f^0	the equilibrium enthalpy of fusion
Δt_{inc}	incubation period or time period which the polymer is still in the molten state
Δt_c	crystallization time
T_{onset}	the actual temperature where the sample began to crystallize

t_{θ}	crystallization time at an arbitrary relative crystallinity
$t_{0.01}$	crystallization time at relative crystallinity equal to 0.01
$t_{0.99}$	crystallization time at relative crystallinity equal to 0.99
$t_{0.5}$	crystallization time at relative crystallinity equal to 0.5 or crystallization half-time
$t_{0.5}^{-1}$	reciprocal crystallization half-time